Electrical Power and Energy Systems 55 (2014) 29–40

Contents lists available at ScienceDirect

Electrical Power and Energy Systems

journal homepage: www.elsevier.com/locate/ijepes

Solution of reactive power dispatch of power systems by an opposition-based gravitational search algorithm ☆

Binod Shaw [a], V. Mukherjee [b,*], S.P. Ghoshal [c]

[a] Department of Electrical Engineering, Asansol Engineering College, Asansol, West Bengal, India
[b] Department of Electrical Engineering, Indian School of Mines, Dhanbad, Jharkhand, India
[c] Department of Electrical Engineering, National Institute of Technology, Durgapur, West Bengal, India

ARTICLE INFO

Article history:
Received 4 February 2013
Received in revised form 10 June 2013
Accepted 21 August 2013

Keywords:
Gravitational search algorithm
Opposition-based learning
Optimal reactive power dispatch
Power systems
Optimization

ABSTRACT

Gravitational search algorithm (GSA) is based on law of gravity and the interaction between masses. In GSA, searcher agents are collection of masses and their interactions are based on Newtonian laws of gravity and motion. In this paper, to further improve the optimization performance of GSA, opposition-based learning is employed in opposition-based gravitational search algorithm (OGSA) for population initialization and also for generation jumping. In the present work, OGSA is applied for the solution of optimal reactive power dispatch (ORPD) of power systems. Traditionally, ORPD is defined as the minimization of active power transmission losses by controlling a number of control variables. ORPD is formulated as a non-linear constrained optimization problem with continuous and discrete variables. In this work, OGSA is used to find the settings of control variables such as generator voltages, tap positions of tap changing transformers and amount of reactive compensation to optimize certain objectives. The study is implemented on IEEE 30-, 57- and 118-bus test power systems with different objectives that reflect minimization of either active power loss or that of total voltage deviation or improvement of voltage stability index. The obtained results are compared to those yielded by the other evolutionary optimization techniques surfaced in the recent state-of-the-art literature including basic GSA. The results presented in this paper demonstrate the potential of the proposed approach and show its effectiveness and robustness for solving ORPD problems of power systems.

1. Introduction

In power systems, basic objective of optimal reactive power dispatch (ORPD) is to identify optimal setting of control variables which minimize the given objective function as either total transmission line loss (P_{Loss}), or absolute value of total voltage deviation (TVD), or improvement of voltage stability index (VSI) while satisfying the unit and system constraints. This goal is accomplished by proper adjustment of reactive power variables like generator voltage magnitudes, transformer tap settings and switchable VAR sources [1].

Several classical gradient-based optimization algorithms [2–6] have been applied to solve different ORPD problems of power systems. These techniques are, computationally, fast. However, conventional optimization techniques like lambda iteration method, linear programming, interior point method, reduced gradient method and Newton method rely heavily on the convexity assumption of generators' cost functions and, usually, approximate these curves using quadratic or piecewise quadratic, monotonically increasing cost function [2,3]. These techniques have difficulties in handling problems with the nonconvex or discontinuous landscape and discrete variables. Ref. [7] may be referred for further discussion on these techniques. Hence, it becomes essential to develop optimization techniques that are capable of overcoming these drawbacks.

In the past, computational intelligence-based techniques, such as genetic algorithm (GA) [8], improved GA [9], real parameter GA [10], adaptive GA [11], evolutionary programming (EP) [12], particle swarm optimization (PSO) [13], hybrid PSO [14], bacterial foraging optimization (BFO) [15], differential evolution (DE) [16–18], seeker optimization algorithm (SOA) [19], gravitational search algorithm (GSA) [20] etc have been applied for solving ORPD problem. These techniques have shown effectiveness in overcoming the disadvantages of classical algorithms. Specially, PSO and DE have received increased attention from researchers because of their novelty and searching capability. However, it does not mean that these techniques do not have any limitations. In solving complex multimodal problems, these methods may be easily trapped into local optima. Furthermore, their searching performance depends on the appropriate parameter settings [21].

* Corresponding author. Tel.: +91 0326 2235644; fax: +91 0326 2296563.
E-mail addresses: binodshaw2000@gmail.com (B. Shaw), vivek_agamani@yahoo.com (V. Mukherjee), spghoshalnitdgp@gmail.com (S.P. Ghoshal).

0142-0615/$ - see front matter © 2013 The Authors. Published by Elsevier Ltd. All rights reserved.
http://dx.doi.org/10.1016/j.ijepes.2013.08.010

Premature convergence and local stagnation are frequently observed in many applications [22].

Rashedi et al. proposes gravitational search algorithm (GSA) in [23]. It is a heuristic evolutionary optimization algorithm based on the metaphor of gravitational interactions between masses. GSA is inspired by the theory of Newton that postulates *every particle in the universe attracts every other particle with a force that is directly proportional to the product of their masses and inversely proportional to the square of the distance between them*.

Tizhoosh introduced the concept of *opposition-based learning* (OBL) in [24]. The main idea behind OBL is simultaneous consideration of an estimate and its corresponding opposite estimate (i.e., guess and opposite guess) in order to achieve a better approximation for the current candidate solution. In the recent literature, the concept of opposite numbers has been utilized to speed up the convergence rate of an optimization algorithm such as opposition-based DE [25]. In opposition-based GSA (OGSA) [26], the same idea of opposite number is blended with GSA for population initialization and also for generating new population. Thus, GSA approach is based on the Newtonian physical law of gravity and law of motion while in OGSA the concept of OBL is employed for population initialization and also for generation jumping [27].

In this work, OGSA is applied for the solution of ORPD problem of power systems. Three IEEE standard power systems like IEEE 30-, 57- and 118-bus power systems are adopted and the ORPD problem of these test power systems are solved with different objectives that reflect minimization of either P_{Loss} or that of TVD or improvement of VSI. Results obtained are compared to other computational intelligence-based meta-heurists surfaced in the recent state-of-the-art literature including basic GSA.

The rest of this paper is organized as follows: In Section 2, mathematical problem of ORPD is stated. In Section 3, OGSA is described. In Section 4, implementation of OGSA for ORPD problem is presented. In Section 5, simulation results are presented and discussed. Finally, conclusion of the present work is drawn in Section 6.

2. Mathematical problem formulation

Mathematical problem of the present work is either minimization of P_{Loss} or that of TVD or improvement of VSI. These three objectives are described in the next three sub-sections followed by constraint handling mechanism for the ORPD problem.

2.1. Minimization of real power loss

The objective of the reactive power optimization is to minimize the active power loss in the transmission network, which can be defined as follows [19]

$$\textit{Minimize}\quad P_{Loss} = f\left(\vec{X}_1, \vec{X}_2\right) = \sum_{k\in N_E} g_k\left(V_i^2 + V_j^2 - 2V_iV_j\cos\theta_{ij}\right) \tag{1}$$

subject to

$$\left.\begin{aligned}
&P_{G_i} - P_{D_i} = V_i\sum_{j\in N_i} V_j(G_{ij}\cos\theta_{ij} + B_{ij}\sin\theta_{ij}) && i\in N_0\\
&Q_{G_i} - Q_{D_i} = V_i\sum_{j\in N_i} V_j(G_{ij}\sin\theta_{ij} - B_{ij}\cos\theta_{ij}) && i\in N_{PQ}\\
&V_i^{\min} \leqslant V_i \leqslant V_i^{\max} && i\in N_B\\
&T_k^{\min} \leqslant T_k \leqslant T_k^{\max} && k\in N_T\\
&Q_{G_i}^{\min} \leqslant Q_{G_i} \leqslant Q_{G_i}^{\max} && i\in N_G\\
&Q_{C_i}^{\min} \leqslant Q_{C_i} \leqslant Q_{C_i}^{\max} && i\in N_C\\
&S_l \leqslant S_l^{\max} && l\in N_l
\end{aligned}\right\} \tag{2}$$

where $f(\vec{X}_1, \vec{X}_2)$ denotes the active power loss function of the transmission network; $\vec{X}_1$ is the control variable vector $[V_G \quad T_k \quad Q_C]^T$; $\vec{X}_2$ is the dependent variable vector; V_G is the generator voltage vector (continuous) except the slack bus voltage; T_k is the transformer tap vector (integer); Q_C is the shunt capacitor/inductor vector (integer); V_L is the load bus voltage vector; Q_G is the generator reactive power vector; $k = (i, j)$, $i \in N_B$, $j \in N_i$ g_k is the conductance of branch k; θ_{ij} is the voltage angle difference between buses i and j; P_{G_i} is the injected active power at bus i; P_{D_i} is the demanded active power at bus i; V_i is the voltage at bus i; G_{ij} is the transfer conductance between bus i and j; B_{ij} is the transfer susceptance between buses i and j; Q_{G_i} is the injected reactive power at bus i; Q_{D_i} is the demanded reactive power at bus i; N_E is the of number of network branches; N_{PQ} is the of number of PQ buses; N_B is the of number of total buses; N_i is the set of numbers of buses adjacent to bus i (including bus i); N_0 is the of number of total buses excluding slack bus; N_C is the of number of possible reactive power source installation buses; N_G is the of number of generator buses; N_T is the of number of transformer branches; S_l is the power flow in branch l; the superscripts "min" and "max" in (2) denote the corresponding lower and upper limits, respectively.

2.2. Minimization of TVD

Treating the bus voltage limits as constraints in ORPD often results in all the voltages toward their maximum limits after optimization, which means the power system lacks the required reserves to provide reactive power during contingencies. One of the effective ways to avoid this situation is to choose the minimization of the absolute deviations of all the actual bus voltages from their desired voltages as an objective function. Minimization of TVD of load buses can allow the improvement of voltage profile [1]. In this case, the power system operates more securely and there will be an increase in service quality. This objective function may be formulated as follows

$$\textit{Minimize}\quad TVD = \sum_{i\in N_L} |V_i - V_i^{ref}| \tag{3}$$

where N_L is the number of load buses in the power system and V_i^{ref} is the desired value of the voltage magnitude of the ith bus which is equal to 1.0 p.u.

2.3. Improvement of VSI

Voltage stability is the ability of a power system to maintain constantly acceptable bus voltage at each bus in the power systems under nominal operating conditions. A system experiences a state of voltage instability when the system is being subjected to a disturbance, or rise in load demand, or change in system configuration. Enhancing voltage stability may be achieved through minimizing the voltage stability indicator L-index values at every bus of the system and consequently the global power system L-index [16]. Voltage stability problem has a close relationship with the reactive power of the system. Voltage stability may be improved by minimizing the voltage stability indicator L-index. In order to enhance the voltage stability and move the system far from the voltage collapse point, improvement of the voltage stability margin is used as an objective for ORPD problem. The VSI objective may, mathematically, be expressed as:

$$L = \min(L_{\max}) = \min[\max(L_k)] \quad \text{where } k = 1, 2, \ldots, N_L \tag{4}$$

where L_k is the voltage stability indicator (L-index) of the kth node and may be formulated as [10]:

$$L_k = \left|1 - \sum_{i\in N_G} F_{ji}\frac{V_i}{V_j}\angle\{\alpha_{ij} + (\delta_i - \delta_j)\}\right| \tag{5}$$

where F_{ji} is the (i,j)th components of the sub matrix obtained by the partial inversion of Y_{Bus} and is given by [16]:

$$F_{ji} = -\left[Y_{jj}\right]^{-1}[Y_{ji}] \tag{6}$$

where Y_{jj} is the self-admittance of the jth bus; Y_{ji} is the mutual admittance between the jth bus and the ith bus; α_{ij} is the phase angle of the term F_{ij}; δ_i, δ_j are the phase angle of the ith and the jth bus voltages, respectively.

2.4. Handling of constraints

It is worth mentioning that during the process of optimization, all the constraints are satisfied as explained below [1].

(a) The load flow equality constraints are satisfied by power flow algorithm.
(b) The generator bus voltage (V_{G_i}), transformer tap setting (T_k) and switchable reactive power compensations (Q_{C_i}) are optimization variables and these are self-restricted between their respective minimum and maximum values by the algorithm.
(c) The limits on active power generation at the slack bus ($P_{G_{slack}}$), load bus voltages (V_{L_i}), reactive power generation (Q_{G_i}) and transmission line flow (S_{l_i}) are state variables. These are restricted by adding a penalty function to the objective function.

3. Description of OGSA

3.1. A brief description of GSA

GSA [23] is navigated by properly adjusting gravitational and inertial masses. In Physics, gravitation is the tendency of objects with mass to accelerate towards each other. In Newton's law of gravity, each particle attracts every other particle with a force known as *gravitational force*. GSA is one of the newest heuristic algorithms that have been inspired by Newton's law of gravity and motion.

In GSA, agents are considered as objects and their performances are measured by their masses. All these objects attract each other by the gravity forces and these forces result a global movement of all the objects towards the objects with heavier masses [28]. Hence, masses cooperate using a direct form of communication through gravitational force. The heavier masses (which correspond to good solutions) move more slowly than the lighter ones. This guarantees exploitation step of the algorithm.

To describe the GSA, consider a system with N_p masses in which position of the ith mass is defined as in (7)

$$X_i = (x_i^1, \ldots, x_i^d \ldots, x_i^n) \quad \text{for } i = 1, 2, \ldots, N_p \tag{7}$$

where x_i^d is position of the ith mass in the dth dimension and n is the dimension of the search space. Based on GSA, mass of each agent is calculated after computing current population's fitness given in (8), (9)

$$m_i(t) = \frac{fit_i(t) - worst(t)}{best(t) - worst(t)} \tag{8}$$

$$M_i(t) = \frac{m_i(t)}{\sum_{i=1}^{Np} m_i(t)} \tag{9}$$

where $M_i(t)$ and $fit_i(t)$ represent the mass and the fitness value of the agent i at t, respectively, and for a minimization problem $worst(t)$ and $best(t)$ are defined in (10), (11).

$$best(t) = \min_{i\in\{1,\ldots,Np\}} fit_i(t) \tag{10}$$

$$worst(t) = \max_{i\in\{1,\ldots,Np\}} fit_i(t) \tag{11}$$

Total forces applied on an agent from a set of heavier masses should be considered based on the law of gravity as stated in (12) which is followed by calculation of acceleration using the law of motion as presented in (13). Afterwards, next velocity of an agent, (as given in (14)), is calculated as a fraction of its current velocity added to its acceleration. Then, its next position may be calculated by using (15).

$$F_i^n(t) = \sum_{j\in Kbest, j\neq i}^{Np} rand_j \times G(t) \times \frac{M_i(t) \times M_j(t)}{R_{ij}(t) + \varepsilon} \times \left(x_j^n(t) - x_i^n(t)\right) \tag{12}$$

$$a_i^n(t) = \frac{F_i^n(t)}{M_i(t)} = \sum_{j\in Kbest, j\neq i}^{Np} rand_j \times G(t) \times \frac{M_j(t)}{R_{ij}(t) + \varepsilon} \times \left(x_j^n(t) - x_i^n(t)\right) \tag{13}$$

$$v_i^n(t+1) = rand_i \times v_i^n(t) + a_i^n(t) \tag{14}$$

$$x_i^n(t+1) = x_i^n(t) + v_i^n(t+1) \tag{15}$$

In (13)–(15), $rand_i$ and $rand_j$ are two uniformly distributed random numbers in the interval $[0,1]$, ε is a small value, $R_{ij}(t)$ is the Euclidean distance between two agents i and j (defined as $R_{ij}(t) = \|x_i(t), x_j(t)\|_2$) and $Kbest$ is the set of first K agents with the best fitness value and biggest mass which is a function of time (initialized to K_0 at the beginning and decreases with time). Here, K_0 is set to N_p (total number of agents) and is decreased linearly to 1. In GSA, the gravitational constant (G) will take an initial value (G_0), and it will be reduced with time as given in (16)

$$G(t) = G_0 \times e^{-\tau\left(\frac{iter}{iter_{\max}}\right)} \tag{16}$$

where G_0 is set to 100, τ is set to 10, $iter$ and $iter_{\max}$ are the current and the total number of iterations (the total age of the system), respectively. The steps of the GSA are depicted below.

Steps of GSA	
Step 1	Population-based initialization
Step 2	Fitness evaluation of the agents
Step 3	Update $M_i(t)$ based on (8), (9), $best(t)$ based on (10) $worst(t)$ based on (11) and $G(t)$ based on (16) for $i = 1, 2, \ldots, N_p$
Step 4	Calculation of total forces in different directions by using (12)
Step 5	Calculation of acceleration by (13) and velocity by (14)
Step 6	Updating agents' positions by (15)
Step 7	Check for the constraints of the problem
Step 8	Repeat steps 2 to 7 until a stopping criterion is met

3.2. Review of GSA-based works

Since its inception in 2009, GSA is being hybridized by the researchers' pool with an aim to have improved optimization performance. Refs. [29–31] may be recalled as just a few towards the attainment of this specific goal. Recently, GSA algorithm has captured much attention and has been, successfully, applied to solve a wide range of practical optimization problems such as edge detection [32,33], filter modeling [34], parameters identification

of hydraulic turbine governing system [35], fuzzy controllers for servo systems [36], forecasting future oil demand [37], robust design of multimachine power system stabilizers [38], solution of ORPD [20] and so on.

3.3. Opposition-based learning: a concept

Evolutionary optimizations methods start with some initial solutions (initial population) and try to improve them toward some optimal solution(s). The process of searching terminates when some predefined criteria are satisfied. We, usually, start with *random guesses* in the absence of *a priori* information about the solution. The computation time, among others, is related to the distance of these initial guesses from the optimal solution. We may improve our chance of starting with a closer (fitter) solution by simultaneously checking *the opposite solution* [24,25]. By doing this, the fitter one (guess or opposite guess) may be chosen as an initial solution. In fact, according to the theory of probability, for 50% of the time, a guess is further away from the solution than its opposite guess. Therefore, starting with the closer of the two guesses (as judged by its fitness) has the potential to accelerate convergence. The same approach may be applied not only to the initial solutions but also continuously to each solution in the current population.

3.3.1. Definition of opposite number

Let $y \in [L, U]$ be a real number. The opposite number is defined by (17)

$$\breve{y} = L + U - y \tag{17}$$

Similarly, this definition can be extended to higher dimensions [24,25] as stated in the next sub-section.

3.3.2. Definition of opposite point

Let $Y = (y_1^1, \ldots y_1^d \ldots, y_1^n)$ be a point in n-dimensional space, where $\{y_1^1, \ldots y_1^d \ldots, y_1^n\} \in R$ and $y_i \in [L, U] \forall_i \in \{1, \ldots, d, \ldots, n\}$. The opposite point $\breve{Y} = (Y_1^1, \ldots \breve{Y}_1^d \ldots Y_1^n)$ is completely defined by its components as stated in (18).

$$\breve{y}_i = L + U - y_i \tag{18}$$

Now, by employing the opposite point definition, the opposition-based optimization is defined in the next sub-section.

3.3.3. Opposition-based optimization

Let $Y = (y_1^1, \ldots y_1^d \ldots, y_1^n)$ be a point in n-dimensional space (i.e., a candidate solution). Assume $f = (.)$ is a fitness function which is used to measure the candidate's fitness. According to the definition of the opposite point, $\breve{Y} = (\breve{y}_1^1, \ldots, \breve{y}_1^d, \ldots, \breve{y}_1^n)$ is the opposite of $Y = (y_1^1, \ldots, y_1^d, \ldots, y_1^n)$ [24,25]. Now, if $f(\breve{Y}) \leqslant f(Y)$ (for a minimization problem), then the point Y can be replaced with $\breve{Y}$ otherwise, we continue with Y. Hence, the point and its opposite point are evaluated simultaneously in order to continue with the fitter one.

3.4. OGSA

Similar to other population-based optimization algorithms, two main steps are distinguishable for GSA. These two are population initialization and producing new generations by adopting the principle of GSA. In the present work, the strategy of OBL [24,25] is incorporated in two steps. The original GSA is chosen as the parent algorithm and opposition-based ideas of [24,25] are embedded in it. Corresponding pseudo code of the proposed OGSA is presented below.

Steps of OGSA

Step 1 Opposition-based population initialization. Generate uniformly distributed initial population P_0
  for ($i = 0; i < N_p; i$ ++) N_p: Population size
    for ($j = 0; j < n; j$ + +) //n: Problem dimension
      $OP_{0_{i,j}} = L_j + U_j - P_{0_{i,j}}$ // OP_0: Opposite of initial population P_0
      //$[L_j, U_j]$: Range of the jth variable
    end for
  end for
  Select N_p fittest individuals from set of $\{P_0, OP_0\}$ as initial population P_0
  End of opposition-based population initialization

Step 2 Fitness evaluation of the agents

Step 3 Update $M_i(t)$ based on (8), (9), $best(t)$ based on (10), and $worst(t)$ based on (11), and $G(t)$ based on (16) for $i = 1, 2, \ldots, N_p$

Step 4 Calculation of total forces in different directions by using (12)

Step 5 Calculation of acceleration by (13) and velocity by (14)

Step 6 Updating agents' positions by (15)

Step 7 Check for the constraints of the problem

Step 8 Opposition based generation jumping
  if ($rand(0, 1) < J_r$) // $rand(0, 1)$: Uniformly generated random number, J_r: Jumping rate
    for ($i = 0; i < N_p; i$ + +)
      for ($j = 0; j < n; j$ + +)
        $OP_{i,j} = \min_j^p + \max_j^p - P_{i,j}$
        // $\min_j^p$:minimum value of the jth variable in the current population (p)
        // $\max_j^p$:maximum value of the jth variable in the current population (p)
      end for
    end for
  end if
  Select N_p fittest individuals from set of $\{P, OP\}$ as current population P
  End of opposition-based generation jumping

Step 9 Repeat steps 2 to 8 until a stopping criterion is met

4. Implementation of OGSA for ORPD problem

The fitness value of each agent is calculated by using the objective function of the problem. The real-value position of the agent

Table 1
Description of test systems.

Description	IEEE 30-bus	IEEE 57-bus	IEEE 118-bus
Buses, N_B	30	57	118
Generators, N_G	6	7	54
Transformers, N_T	4	15	9
Shunts, N_Q	9	3	14
Branches, N_E	41	80	186
Equality constraints	60	114	236
Inequality constraints	125	245	572
Control variables	19	27	77
Discrete variables	6	20	21
Base case for P_{Loss}, MW	5.660	27.8637	132.4500
Base case for TVD, p.u.	0.58217	1.23358	1.439337

consists of three parts: generator voltages, transformer taps and shunt capacitors/inductors. The real-value position of the agents is changed into a mixed-variable vector which is used to calculate the objective function value of the problem based on Newton–Raphson power flow analysis [39]. The reactive power optimization based on OGSA may be described as follows.

OGSA Algorithm for ORPD problem

Step 1	Read the parameters of power system and those of OGSA and specify the lower and upper limits of each variable
Step 2	Population-based initialization (P_0)
Step 3	Opposition-based population initialization (OP_0)
Step 4	Select N_p fittest individuals from set of $\{P_0, OP_0\}$ as initial population P_0
Step 5	Fitness evaluation of the agents using the objective function of the problem based on the results of Newton–Raphson power flow analysis [39]
Step 6	Update $M_i(t)$ based on (8), (9), $best(t)$ based on (10), and $worst(t)$ based on (11), and $G(t)$ based on (16) for $i = 1, 2, \ldots, N_p$
Step 7	Calculation of the total forces in different directions by using (12)
Step 8	Calculation of acceleration by (13) and the velocity by (14)
Step 9	Updating agents' positions by (15)
Step 10	Check for the constraints of the problem
Step 11	Opposition based generation jumping
Step 12	Go to Step 5 until a stopping criterion is satisfied

5. Simulation results and discussions

In the present work, OGSA is applied to IEEE 30-, 57- and 118-bus standard test power systems for the solution of ORPD problems. Description of these studied test systems is depicted in Table 1. The software is written in MATLAB 2008a computing environment and applied on a 2.63 GHz Pentium IV personal computer with 3 GB RAM. The value of G_0 is set to 100 and τ is set to 10 [20]. The value of J_r is selected as 0.3 (Explanation is given in Section 5.4). Number of fitness function evaluations (NFFEs) is set to 1000 for all the test cases. Discussions on simulation results of the present work are presented below. Results of interest are **bold faced** in the respective tables to indicate the optimization capability of the proposed OGSA algorithm. In this study, 30/100 test runs are performed for all the test cases to solve the ORPD problem and the best results are presented.

5.1. Test system 1: IEEE 30-bus power system

IEEE 30-bus power system is taken as test system 1. Generator data, load data, line data, minimum and maximum limits for active power sources, bus voltages, tap settings and reactive power sources for this test system are taken from [20]. This test system has nineteen control variables and these are six generator voltage magnitudes (at the buses 1, 2, 5, 8, 11 and 13), four transformers with off-nominal tap ratio (at lines 6–9, 6–10, 4–12 and 28–27) and nine shunt VAR compensation devices (at buses 10, 12, 15, 17, 20, 21, 23, 24 and 29). The total system demand is 2.834 p.u. at 100 MVA base.

5.1.1. Minimization of system P_{Loss} for IEEE 30-bus power system

The proposed approach is applied for minimization of P_{Loss} as one of the objective function. The obtained optimal values of control variables, as obtained from the proposed OGSA method, are given in Table 2. The results obtained by the proposed OGSA are compared to those reported in the literature like GSA [20], biogeography-based optimization (BBO) [40], DE [16], comprehensive learning PSO (CLPSO) [41], PSO [41] and self-adaptive real coded GA (SARGA) [42]. The obtained minimum P_{Loss} from the proposed approach is **4.4984 MW**. The value of P_{Loss} yielded by OGSA is less by **0.01591 MW** (i.e. **0.3524%**) compared to GSA-based best results of 4.514310 MW. Comparative GA-, PSO- and OGSA-based convergence profiles of P_{Loss} (MW) for this test power system is presented

Table 2
Comparison of simulation results for IEEE 30-bus test power system with P_{Loss} minimization objective.

Variable	OGSA	GSA [20]	BBO [40]	DE [16]	CLPSO [41]	PSO [41]	SARGA [42]
Generator voltage							
V_1, p.u.	1.0500	1.071652	1.1000	1.1000	1.1000	1.1000	NR*
V_2, p.u.	1.0410	1.022199	1.0944	1.0931	1.1000	1.1000	NR*
V_5, p.u.	1.0154	1.040094	1.0749	1.0736	1.0795	1.0867	NR*
V_8, p.u.	1.0267	1.050721	1.0768	1.0756	1.1000	1.1000	NR*
V_{11}, p.u.	1.0082	0.977122	1.0999	1.1000	1.1000	1.1000	NR*
V_{13}, p.u.	1.0500	0.967650	1.0999	1.1000	1.1000	1.1000	NR*
Transformer tap ratio							
T_{6-9}	1.0585	1.098450	1.0435	1.0465	0.9154	0.9587	NR*
T_{6-10}	0.9089	0.982481	0.90117	0.9097	0.9000	1.0543	NR*
T_{4-12}	1.0141	1.095909	0.98244	0.9867	0.9000	1.0024	NR*
T_{28-27}	1.0182	1.059339	0.96918	0.9689	0.9397	0.9755	NR*
Capacitor banks							
Q_{C-10}, p.u.	0.0330	1.653790	4.9998	5.0000	4.9265	4.2803	NR*
Q_{C-12}, p.u.	0.0249	4.372261	4.987	5.0000	5.0000	5.0000	NR*
Q_{C-15}, p.u.	0.0177	0.119957	4.9906	5.0000	5.0000	3.0288	NR*
Q_{C-17}, p.u.	0.0500	2.087617	4.997	5.0000	5.0000	4.0365	NR*
Q_{C-20}, p.u.	0.0334	0.357729	4.9901	4.4060	5.0000	2.6697	NR*
Q_{C-21}, p.u.	0.0403	0.260254	4.9946	5.0000	5.0000	3.8894	NR*
Q_{C-23}, p.u.	0.0269	0.000000	3.8753	2.8004	5.0000	0.0000	NR*
Q_{C-24}, p.u.	0.0500	1.383953	4.9867	5.0000	5.0000	3.5879	NR*
Q_{C-29}, p.u.	0.0194	0.000317	2.9098	2.5979	5.0000	2.8415	NR*
P_{Loss}, MW	**4.4984**	4.514310	4.5511	4.5550	4.5615	4.6282	4.57401
TVD, p.u.	0.8085	0.875220	NR*	1.9589	0.4773	1.0883	NR*
L-index, p.u.	0.1407	0.141090	NR*	0.5513	NR*	NR*	NR*
CPU time, s	89.19	94.6938	NR*	NR*	138	130	NR*

NR* means not reported.

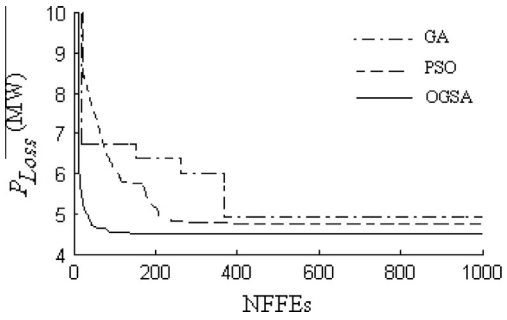

Fig. 1. Comparative convergence profiles of transmission loss for IEEE 30-bus test power system.

in Fig. 1. From this figure it may be observed that the convergence profile of P_{Loss} (MW) for the proposed OGSA-based approach for this test system is promising one. The computational times of the compared algorithms are also shown in Table 2. It may be seen from this table that the computing time of OGSA is less than other evolutionary meta-heuristics including the basic GSA reported in [20].

5.1.2. Minimization of system TVD for IEEE 30-bus power system

The proposed OGSA-based approach is also applied for the minimization of TVD of this test power network. The results yielded by the proposed OGSA-based approach are presented in Table 3. The results obtained by the proposed OGSA are compared to those reported in the literature like GSA [20] and DE [16]. From this table, **5.37%** improvement in TVD may be recorded by using the proposed OGSA-based algorithm as compared to GSA counterpart as reported in [20]. Comparative GA-, PSO- and OGSA-based convergence profiles of TVD (p.u.) for this test power system is presented in Fig. 2. From this figure it may be observed that the convergence profile of TVD (p.u.) for the proposed OGSA-based approach for this test system is promising one.

Table 3
Comparison of simulation results for IEEE 30-bus test power system with (a) TVD minimization objective and (b) improvement of VSI.

Variable	(a) TVD minimization			(b) Improvement of VSI		
	OGSA	GSA [20]	DE [16]	OGSA	GSA [20]	DE [16]
Generator voltage						
V_1, p.u.	0.9746	0.983850	1.0100	1.0951	1.100000	1.0993
V_2, p.u.	1.0273	1.044807	0.9918	1.0994	1.100000	1.0967
V_5, p.u.	0.9965	1.020353	1.0179	1.0991	1.100000	1.0990
V_8, p.u.	0.9982	0.999126	1.0183	1.0991	1.100000	1.0346
V_{11}, p.u.	0.9826	1.077000	1.0114	1.0995	1.100000	1.0993
V_{13}, p.u.	1.0403	1.043932	1.0282	1.0994	1.100000	0.9517
Transformer tap ratio						
T_{6-9}	0.9909	0.900000	1.0265	0.9728	0.900000	0.9038
T_{6-10}	1.0629	1.100000	0.9038	0.9000	0.900000	0.9029
T_{4-12}	1.0762	1.050599	1.0114	0.9534	0.900000	0.9002
T_{28-27}	1.0117	0.961999	0.9635	0.9501	1.019538	0.9360
Capacitor banks						
Q_{C-10}, p.u.	0.0246	0.000000	4.9420	0.0021	5.000000	0.6854
Q_{C-12}, p.u.	0.0175	0.473512	1.0885	0.0265	5.000000	4.7163
Q_{C-15}, p.u.	0.0283	5.000000	4.9985	0.0000	5.000000	4.4931
Q_{C-17}, p.u.	0.0403	0.000000	0.2393	0.0006	5.000000	4.5100
Q_{C-20}, p.u.	0.0000	5.000000	4.9958	0.0000	5.000000	4.4766
Q_{C-21}, p.u.	0.0270	0.000000	4.9075	0.0000	5.000000	4.6075
Q_{C-23}, p.u.	0.0385	4.999834	4.9863	0.0000	5.000000	3.8806
Q_{C-24}, p.u.	0.0257	5.000000	4.9663	0.0009	5.000000	3.8806
Q_{C-29}, p.u.	0.0000	5.000000	2.2325	0.000	5.000000	3.2541
P_{Loss}, MW	6.9044	6.911765	6.4755	5.9198	4.975298	7.0733
TVD, p.u.	**0.0640**	0.067633	0.0911	1.9887	0.215793	1.419
L-index, p.u.	0.13381	0.134937	0.5734	**0.1230**	0.136844	0.1246
CPU time, s	190.14	198.6532	NR*	185.16	NR*	NR*

NR* means not reported.

5.1.3. Improvement of VSI for IEEE 30-bus power system

Results obtained by the proposed OGSA algorithm for the improvement of voltage stability index for IEEE 30-bus test power system are also presented in Table 3. The results obtained by the proposed OGSA are compared to those reported in the literature like GSA [20] and DE [16]. From this table, **10.11%** improvement in voltage stability index may be recorded by using the proposed OGSA-based algorithm as compared to GSA reported in [20]. Comparative GA-, PSO- and OGSA-based convergence profiles of VSI for this test power system is presented in Fig. 3. From this figure it may be observed that the convergence profile of voltage stability index for the proposed OGSA-based approach for this test system is promising one.

5.2. Test system 2: IEEE 57-bus power system

The standard IEEE 57-bus system consists of eighty transmission lines, seven generators (at the buses 1, 2, 3, 6, 8, 9, 12) and fifteen branches under load tap setting transformer branches is taken as test system 2. There reactive power sources are considered at buses 18, 25 and 53. Line data, bus data, variable limits and the initial values of the control variables are taken from [43,44]. The search space of this case system has twenty five dimensions, including seven generator voltages, fifteen transformer taps and three reactive power sources. The system loads are given as follows: P_{Load} = 12.508 p.u., Q_{Load} = 3.364 p.u. The initial total generations and power losses are: P_G = 12.7926 p.u., Q_G = 3.4545 p.u., P_{Loss} = 0.28462 p.u., Q_{Loss} = −1.2427 p.u. There are five bus voltages in p.u. outside the limits: V_{25} = 0.938, V_{30} = 0.920, V_{31} = 0.900, V_{32} = 0.926, V_{33} = 0.924.

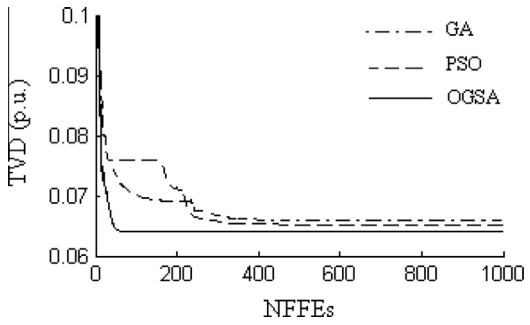

Fig. 2. Comparative convergence profiles of TVD for IEEE 30-bus test power system.

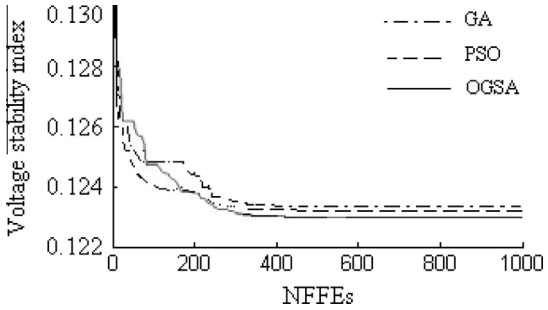

Fig. 3. Comparative convergence profiles of voltage stability index for IEEE 30-bus test power system.

5.2.1. Minimization of system P_{Loss} for IEEE 57-bus power system

Table 4 depicts the solution result for P_{Loss} minimization objective while the best reactive power dispatch solutions for this objective are tabulated in Table 4. In Table 4, OGSA based results are compared to other optimization technique recently reported in the literature like GSA [20]; nonlinear programming (NLP) [19];

Table 4
Comparison of simulation results for IEEE 57-bus test power system with P_{Loss} minimization objective.

Variable	OGSA	GSA [20]	NLP [19]	CGA [19]	AGA [19]	PSO-w [19]	PSO-cf [19]
Generator voltage							
V_1, p.u.	1.0600	1.060000	1.06	0.9686	1.0276	1.06	1.06
V_2, p.u.	1.0594	1.060000	1.06	1.0493	1.0117	1.0578	1.0586
V_3, p.u.	1.0492	1.060000	1.0538	1.0567	1.0335	1.04378	1.0464
V_6, p.u.	1.0433	1.008102	1.06	0.9877	1.0010	1.0356	1.0415
V_8, p.u.	1.0600	1.054955	1.06	1.0223	1.0517	1.0546	1.06
V_9, p.u.	1.0450	1.009801	1.06	0.9918	1.0518	1.0369	1.0423
V_{12}, p.u.	1.0407	1.018591	1.06	1.0044	1.0570	1.0334	1.0371
Transformer tap ratio							
T_{4-18}	0.9000	1.100000	0.91	0.92	1.03	0.90	0.98
T_{4-18}	0.9947	1.082634	1.06	0.92	1.02	1.02	0.98
T_{21-20}	0.9000	0.921987	0.93	0.97	1.06	1.01	1.01
T_{24-26}	0.9001	1.016731	1.08	0.90	0.99	1.01	1.01
T_{7-29}	0.9111	0.996262	1.00	0.91	1.10	0.97	0.98
T_{34-32}	0.9000	1.100000	1.09	1.1	0.98	0.97	0.97
T_{11-41}	0.9000	1.074625	0.92	0.94	1.01	0.90	0.90
T_{15-45}	0.9000	0.954340	0.91	0.95	1.08	0.97	0.97
T_{14-46}	1.0464	0.937722	0.98	1.03	0.94	0.95	0.96
T_{10-51}	0.9875	1.016790	0.98	1.09	0.95	0.96	0.97
T_{13-49}	0.9638	1.052572	0.98	0.90	1.05	0.92	0.93
T_{11-43}	0.9000	1.100000	0.98	0.90	0.95	0.96	0.97
T_{40-56}	0.9000	0.979992	0.98	1.00	1.01	1.00	0.99
T_{39-57}	1.0148	1.024653	1.08	0.96	0.94	0.96	0.96
T_{9-55}	0.9830	1.037316	1.03	1.00	1.00	0.97	0.98
Capacitor banks							
Q_{C-18}, p.u.	0.0682	0.078254	0.08352	0.084	0.0168	0.05136	0.09984
Q_{C-25}, p.u.	0.0590	0.005869	0.00864	0.00816	0.01536	0.05904	0.05904
Q_{C-53}, p.u.	0.0630	0.046872	0.01104	0.05376	0.03888	0.06288	0.06288
P_{Loss}, p.u.	**0.2343**	0.23461194	0.2590231	0.2524411	0.2456484	0.2427052	0.2428022
TVD, p.u.	1.1907	NR*	NR*	NR*	NR*	NR*	NR*
L-index, p.u.	0.4120	NR*	NR*	NR*	NR*	NR*	NR*
CPU time, s	307.39	321.4872	NR*	321.4872	NR*	353.08	404.63

Variable	CLPSO [19]	SPSO-07 [19]	L-DE [19]	L-SACP-DE [19]	L-SaDE [19]	SOA [19]	BBO [40]	BBO* [40]
Generator voltage								
V_1, p.u.	1.0541	1.0596	1.0397	0.9884	1.0600	1.06	1.0600	1.0600
V_2, p.u.	1.0529	1.0580	1.0463	1.0543	1.0574	1.0580	1.0504	1.0580
V_3, p.u.	1.0337	1.0488	1.0511	1.0278	1.0438	1.0437	1.0440	1.0442
V_6, p.u.	1.0313	1.0362	1.0236	0.9672	1.0364	1.0352	1.0376	1.0364
V_8, p.u.	1.0496	1.06	1.0538	1.0552	1.0537	1.0548	1.0550	1.0567
V_9, p.u.	1.0302	1.0433	0.94518	1.0245	1.0366	1.0369	1.0229	1.0377
V_{12}, p.u.	1.0342	1.0356	0.99078	1.0098	1.0323	1.0336	1.0323	1.0351
Transformer tap ratio								
T_{4-18}	0.99	0.95	1.02	1.05	0.94	1.00	0.96693	0.99165
T_{4-18}	0.98	0.99	0.91	1.05	1.00	0.96	0.99022	0.96447
T_{21-20}	0.99	0.99	0.97	0.95	1.01	1.01	1.0120	1.0122
T_{24-26}	1.01	1.02	0.91	0.98	1.01	1.01	1.0087	1.0110
T_{7-29}	0.99	0.97	0.96	0.97	0.97	0.97	0.97074	0.97127
T_{34-32}	0.93	0.96	0.99	1.09	0.97	0.97	0.96869	0.97227
T_{11-41}	0.91	0.92	0.98	0.92	0.9	0.90	0.90082	0.90095
T_{15-45}	0.97	0.96	0.96	0.91	0.97	0.97	0.96602	0.97063
T_{14-46}	0.95	0.95	1.05	1.08	0.96	0.95	0.95079	0.95153
T_{10-51}	0.98	0.97	1.07	0.99	0.96	0.96	0.96414	0.96252
T_{13-49}	0.95	0.92	0.99	0.91	0.92	0.92	0.92462	0.92227
T_{11-43}	0.95	1.00	1.06	0.94	0.96	0.96	0.95022	0.95988
T_{40-56}	1.00	1.00	0.99	0.99	1.00	1.00	0.99666	1.0018
T_{39-57}	0.96	0.95	0.97	0.96	0.96	0.96	0.96289	0.96567
T_{9-55}	0.97	0.98	1.07	1.1	0.97	0.97	0.96001	0.97199
Capacitor banks								
Q_{C-18}, p.u.	0.09888	0.03936	0	0	0.08112	0.09984	0.09782	0.09640
Q_{C-25}, p.u.	0.05424	0.05664	0	0	0.05808	0.05904	0.058991	0.05897
Q_{C-53}, p.u.	0.06288	0.03552	0	0	0.06192	0.06288	0.6289	0.062948
P_{Loss}, p.u.	0.2451520	0.2443043	0.2781264	0.2791553	0.2426739	0.2426548	0.24544	0.242616
TVD, p.u.	NR*	NR*	NR*	NR*	NR*	NR*	NR*	NR*
L-index, p.u.	NR*	NR*	NR*	NR*	NR*	NR*	NR*	NR*
CPU time, s	423.30	421.98	426.97	427.23	408.97	382.23	NR*	NR*

BBO* means (after relaxing Q-limit of bus 2 and 9) [40], NR* means not reported.

canonical GA (CGA) [19]; adaptive GA (AGA) [19]; PSO with adaptive inertia weight (PSO-w) [19]; PSO with a constriction factor (PSO-cf) [19]; CLPSO [19]; a "real standard" version of PSO, called as SPSO-07 [19]; DEs with local search, instead of their corresponding original versions and denoted as L-DE [19], L-SACP-DE [19], L-SaDE [19]; SOA [19]; BBO [40]; BBO (after relaxing Q-limit of bus 2 and 9) [40]. From Table 4, it may be observed OGSA based results yield optimal value of P_{Loss} for this power network. In [19], base case power loss for this test power network is reported as 0.28462 p.u. The% P_{Save}in Table 5 denotes the saving percent of the P_{Loss}. Table 5 demonstrates that a power loss reduction of **17.68%** (from 0.28462 p.u. to 0.2343 p.u.) is accomplished by using the proposed OGSA approach, which is the biggest reduction of power loss than that obtained by the other approaches. The total time of taken by the comparative algorithms are summarized in Table 6, which portrays the execution time taken by the proposed OGSA approach for this power network is the least one among the algorithms reported in this table. Comparative GA-, PSO- and OGSA-based convergence profiles of P_{Loss} (MW) for this test power system is presented in Fig. 4. From this figure it may be observed that the convergence profile of P_{Loss} (MW) for the proposed OGSA-based approach for this test system is promising one.

Table 5
The best dispatch solutions (p.u.) for various algorithms on IEEE 57-bus test power system for P_{Loss} minimization objective.

Algorithms	$\sum P_G$ (p.u.)	$\sum Q_G$ (p.u.)	P_{Loss} (p.u.)	Q_{Loss} (p.u.)	% P_{Save}
CGA [19]	12.7752	3.1744	0.267170	−1.1565	6.1308
AGA [19]	12.7661	3.0679	0.258072	−1.1326	9.3276
PSO-w [19]	12.7677	3.1026	0.259729	−1.1598	8.7453
PSO-cf [19]	12.7559	3.0157	0.247866	−1.1137	12.9132
CLPSO [19]	12.7660	3.1501	0.257968	−1.1295	9.3642
SPSO-2007 [19]	12.7822	3.1818	0.274210	−1.2532	3.6576
L-DE [19]	12.7999	3.3656	0.291864	−1.2158	−1.2380
L-SACP-DE [19]	12.7812	3.2085	0.273183	−1.1868	4.0185
L-SaDE [19]	12.7549	3.0191	0.246712	−1.1209	13.2696
SOA [19]	12.7543	2.9837	0.246248	−1.0914	13.4820
GSA [20]	NR*	NR*	0.23461194	NR*	3.31452
OGSA	12.7423	2.916	**0.2343**	−1.0712	**17.68**

NR* means not reported.

Table 6
Computing times for various algorithms on IEEE 57-bus test power system for P_{Loss} minimization objective over 30 runs.

Algorithms	Computing time (s)		
	Shortest	Longest	Average
CGA [19]	1265.34	1295.02	1284.11
AGA [19]	1273.44	1323.91	1293.78
PSO-w [19]	1216.91	1244.64	1229.98
PSO-cf [19]	1188.45	1268.00	1225.14
CLPSO [19]	1399.48	1448.84	1426.19
SPSO-2007 [19]	433.36	495.97	480.94
L-DE [19]	1210.73	1239.86	1224.27
L-SACP-DE [19]	1212.95	1235.03	1221.51
L-SaDE [19]	1273.42	1368.03	1306.86
SOA [19]	1192.83	1288.66	1221.10
GSA [20]	321.4872	NR*	NR*
OGSA	309.12	345.12	315.29

NR* means not reported.

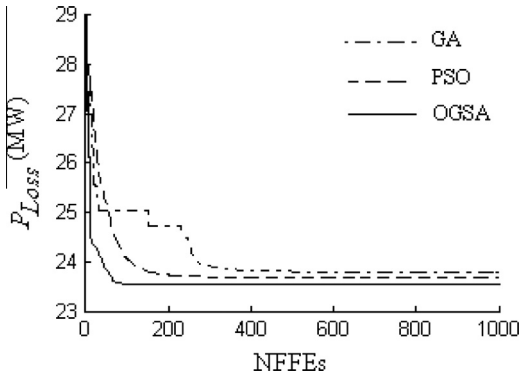

Fig. 4. Comparative convergence profiles of transmission loss for IEEE 57-bus test power system.

Table 7
Comparison of simulation results for IEEE 57-bus test power system with TVD minimization objective.

Variable	OGSA	Variable	OGSA
Generator voltage		T_{15-45}	0.9265
V_1, p.u.	1.0138	T_{14-46}	0.9960
V_2, p.u.	0.9608	T_{10-51}	1.0386
V_3, p.u.	1.0173	T_{13-49}	0.9060
V_6, p.u.	0.9898	T_{11-43}	0.9234
V_8, p.u.	1.0362	T_{40-56}	0.9871
V_9, p.u.	1.0241	T_{39-57}	1.0132
V_{12}, p.u.	1.0136	T_{9-55}	0.9372
Transformer tap ratio		Capacitor banks	
T_{4-18}	0.9833	Q_{C-18}, p.u.	0.0463
T_{4-18}	0.9503	Q_{C-25}, p.u.	0.0590
T_{21-20}	0.9523	Q_{C-53}, p.u.	0.0628
T_{24-26}	1.0036	P_{Loss}, p.u.	0.3234
T_{7-29}	0.9778	TVD, p.u.	**0.6982**
T_{34-32}	0.9146	*L*-index, p.u.	0.5123
T_{11-41}	0.9454	CPU time, s	419.17

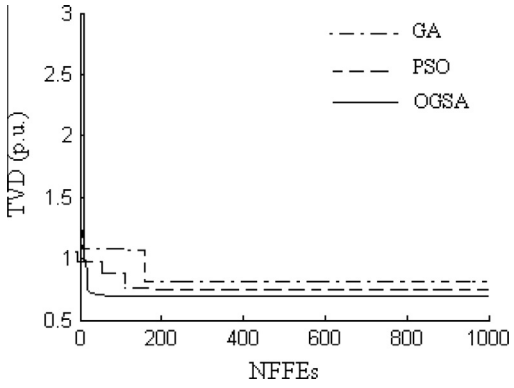

Fig. 5. Comparative convergence profiles of TVD for IEEE 57-bus test power system.

Table 8
Statistical comparison of results of IEEE 57-bus test system with improvement of VSI objective on 30 runs.

Algorithms	*Best* (p.u.)	*Worst* (p.u.)	*Mean* (p.u.)	*Std.*
CGA [19]	0.186249	0.173969	0.1798794	2.4399×10^{-3}
AGA [19]	0.188582	0.180030	0.1848524	2.2259×10^{-3}
PSO-w [19]	0.190745	0.190117	0.1904974	2.1346 × 10−4
PSO-cf [19]	0.190754	0.1870317	0.1895324	122285×10^{-3}
CLPSO [19]	0.187857	0.1783987	0.183922	3.0781×10^{-3}
SPSO-2007 [19]	0.190411	0.182206	0.187245	1.9834×10^{-3}
L-DE [19]	0.1778431	0.165211	0.171368	3.4560×10^{-3}
L-SACP-DE[19]	0.183051	0.159702	0.170998	5.7523×10^{-3}
L-SaDE [19]	0.190638	0.1853272	0.1882648	1.9748×10^{-3}
SOA [19]	0.190709	0.176374	0.187451	2.6388×10^{-3}
OGSA	**0.190010**	0.175935	0.184112	2.8188×10^{-3}

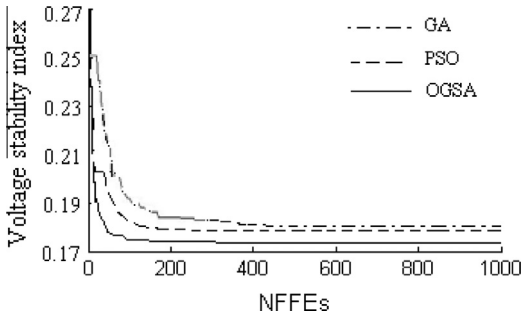

Fig. 6. Comparative convergence profiles of voltage stability index for IEEE 57-bus test power system.

5.2.2. Minimization of system TVD for IEEE 57-bus power system

The best reactive power dispatch solutions as yielded by the proposed OGSA for TVD minimization objective are tabulated in Table 7. Comparative GA-, PSO- and OGSA-based convergence profiles of TVD (p.u.) for this test power system is presented in Fig. 5. From this figure it may be observed that the convergence profile of TVD (p.u.) for the proposed OGSA-based approach for this test system is promising one.

5.2.3. Improvement of VSI for IEEE 57-bus power system

Table 8 presents statistical comparison of the results for improvement of VSI for various algorithms on IEEE 57-bus system over 30 runs. From this table it may be inferred that the proposed OGSA yields better results as compared to the compared algorithms of this table. Comparative GA-, PSO- and OGSA-based convergence profiles of VSI for this test power system is presented in Fig. 6. From this figure it may be observed that the convergence profile of VSI for the proposed OGSA-based approach for this test system is promising one.

5.3. Test system 3: IEEE 118-bus power system

To test the proposed technique in solving ORPD problems of larger power systems, a standard IEEE 118-bus test system is considered as test system 3 [43,45,46]. The search space of this case system has seventy seven dimensions, that is, the fifty four generator buses, sixty four load buses, one hundred eighty six transmission lines, nine transformer taps and fourteen reactive power sources. The system line data, bus data, variable limits and the initial values of control variables are given in [43,45]. The maximum and minimum limits of reactive power sources, bus voltage and

Table 9
Comparison of simulation results for IEEE 118-bus test system with P_{Loss} minimization objective.

Variable	OGSA	GSA [20]	CLPSO[41]	PSO[41]	Variable	OGSA	GSA [20]	CLPSO[41]	PSO [41]
Generator voltage					V_{91}, p.u.	1.0297	1.0032	1.0288	0.9615
V_1, p.u.	1.0350	0.9600	1.0332	1.0853	V_{92}, p.u.	1.0353	1.0927	0.9760	0.9568
V_4, p.u.	1.0554	0.9620	1.0550	1.0420	V_{99}, p.u.	1.0395	1.0433	1.0880	0.9540
V_6, p.u.	1.0301	0.9729	0.9754	1.0805	V_{100}, p.u.	1.0275	1.0786	0.9617	0.9584
V_8, p.u.	1.0175	1.0570	0.9669	0.9683	V_{103}, p.u.	1.0158	1.0266	0.9611	1.0162
V_{10}, p.u.	1.0250	1.0885	0.9811	1.0756	V_{104}, p.u.	1.0165	0.9808	1.0125	1.0992
V_{12}, p.u.	1.0410	0.9630	1.0092	1.0225	V_{105}, p.u.	1.0197	1.0163	1.0684	0.9694
V_{15}, p.u.	0.9973	1.0127	0.9787	1.0786	V_{107}, p.u.	1.0408	0.9987	0.9769	0.9656
V_{18}, p.u.	1.0047	1.0069	1.0799	1.0498	V_{110}, p.u.	1.0288	1.0218	1.0414	1.0873
V_{19}, p.u.	0.9899	1.0003	1.0805	1.0776	V_{111}, p.u.	1.0194	0.9852	0.9790	1.0375
V_{24}, p.u.	1.0287	1.0105	1.0286	1.0827	V_{112}, p.u.	1.0132	0.9500	0.9764	1.0920
V_{25}, p.u.	1.0600	1.0102	1.0307	0.9564	V_{113}, p.u.	1.0386	0.9764	0.9721	1.0753
V_{26}, p.u.	1.0855	1.0401	0.9877	1.0809	V_{116}, p.u.	0.9724	1.0372	1.0330	0.9594
V_{27}, p.u.	1.0081	0.9809	1.0157	1.0874	Transformer tap ratio				
V_{31}, p.u.	0.9948	0.9500	0.9615	0.9608	T_8	0.9568	1.0659	1.0045	1.0112
V_{32}, p.u.	0.9993	0.9552	0.9851	1.1000	T_{32}	1.0409	0.9534	1.0609	1.0906
V_{34}, p.u.	0.9958	0.9910	1.0157	0.9611	T_{36}	0.9963	0.9328	1.0008	1.0033
V_{36}, p.u.	0.9835	1.0091	1.0849	1.0367	T_{51}	0.9775	1.0884	1.0093	1.0000
V_{40}, p.u.	0.9981	0.9505	0.9830	1.0914	T_{93}	0.9560	1.0579	0.9922	1.0080
V_{42}, p.u.	1.0068	0.9500	1.0516	0.9701	T_{95}	0.9956	0.9493	1.0074	1.0326
V_{46}, p.u.	1.0355	0.9814	0.9754	1.0390	T_{102}	0.9882	0.9975	1.0611	0.9443
V_{49}, p.u.	1.0333	1.0444	0.9838	1.0836	T_{107}	0.9251	0.9887	0.9307	0.9067
V_{54}, p.u.	0.9911	1.0379	0.9637	0.9764	T_{127}	1.0661	0.9801	0.9578	0.9673
V_{55}, p.u.	0.9914	0.9907	0.9716	1.0103	Capacitor banks				
V_{56}, p.u.	0.9920	1.0333	1.0250	0.9536	$Q_{C\text{-}5}$, p.u.	−0.3319	0.00	0.0000	0.0000
V_{59}, p.u.	0.9909	1.0099	1.0003	0.9672	$Q_{C\text{-}34}$, p.u	0.0480	7.46	11.7135	9.3639
V_{61}, p.u.	1.0747	1.0925	1.0771	1.0938	$Q_{C\text{-}37}$, p.u.	−0.2490	0.00	0.0000	0.0000
V_{62}, p.u.	1.0753	1.0393	1.0480	1.0978	$Q_{C\text{-}44}$, p.u.	0.0328	6.07	9.8932	9.3078
V_{65}, p.u.	0.9814	0.9998	0.9684	1.0892	$Q_{C\text{-}45}$, p.u.	0.0383	3.33	9.4169	8.6428
V_{66}, p.u.	1.0487	1.0355	0.9648	1.0861	$Q_{C\text{-}46}$, p.u.	0.0545	6.51	2.6719	8.9462
V_{69}, p.u.	1.0490	1.1000	0.9574	0.9665	$Q_{C\text{-}48}$, p.u.	0.0181	4.47	2.8546	11.8092
V_{70}, p.u.	1.0395	1.0992	0.9765	1.0783	$Q_{C\text{-}74}$, p.u.	0.0509	9.72	0.5471	4.6132
V_{72}, p.u.	0.9900	1.0014	1.0243	0.9506	$Q_{C\text{-}79}$, p.u.	0.1104	14.25	14.8532	10.5923
V_{73}, p.u.	1.0547	1.0111	0.9651	0.9722	$Q_{C\text{-}82}$, p.u.	0.0965	17.49	19.4270	16.4544
V_{74}, p.u.	1.0167	1.0476	1.0733	0.9713	$Q_{C\text{-}83}$, p.u.	0.0263	4.28	6.9824	9.6325
V_{76}, p.u.	0.9972	1.0211	1.0302	0.9602	$Q_{C\text{-}105}$, p.u.	0.0442	12.04	9.0291	8.9513
V_{77}, p.u.	1.0071	1.0187	1.0275	1.0781	$Q_{C\text{-}107}$, p.u.	0.0085	2.26	4.9926	5.0426
V_{80}, p.u.	1.0066	1.0462	0.9857	1.0788	$Q_{C\text{-}110}$, p.u.	0.0144	2.94	2.2086	5.5319
V_{85}, p.u.	0.9893	1.0491	0.9836	0.9568	P_{Loss}, MW	**126.99**	127.7603	130.96	131.99
V_{87}, p.u.	0.9693	1.0426	1.0882	0.9642	TVD, p.u.	1.1829	NR*	NR*	NR*
V_{89}, p.u.	1.0527	1.0955	0.9895	0.9748	L-index, p.u.	0.1400	NR*	NR*	NR*
V_{90}, p.u.	1.0290	1.0417	0.9905	1.0248	CPU, s	1152.32	1198.6583	1472	1215

NR*means not reported.

Table 10
Statistical comparison of results of IEEE 118-bus power test system based with P_{Loss} minimization objective on 100 trial runs.

Criterion	PSO [41]	CLPSO [41]	GSA [20]	OGSA
Best solution, MW	131.99	130.96	127.7603	**126.99**
Worst solution, MW	134.5	132.74	NR*	131.99
Median, MW	132.37	131.15	NR*	127.14
Standard deviation	32×10^{-5}	85×10^{-6}	NR*	88×10^{-6}
Success rate, %	59	73	NR*	75
Average CPU time, s	1215	1472	1198.6583	1101.26

NR* means not reported.

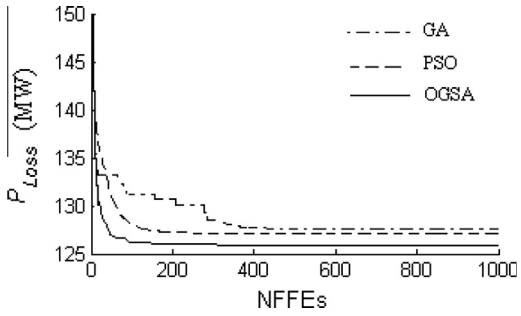

Fig. 7. Comparative convergence profiles of transmission loss for IEEE 118-bus test power system.

Table 11
Comparison of simulation results for IEEE 118-bus test power system with TVD minimization objective.

Variable	OGSA	Variable	OGSA	Variable	OGSA
Generator voltage				Transformer tap ratio	
V_1, p.u.	1.0388	V_{65}, p.u.	0.9724	T_8	0.9841
V_4, p.u.	0.9872	V_{66}, p.u.	1.0020	T_{32}	1.0377
V_6, p.u.	0.9925	V_{69}, p.u.	0.9827	T_{36}	0.9573
V_8, p.u.	0.9905	V_{70}, p.u.	0.9997	T_{51}	0.9952
V_{10}, p.u.	0.9919	V_{72}, p.u.	1.0123	T_{93}	0.9622
V_{12}, p.u.	1.0077	V_{73}, p.u.	0.9960	T_{95}	1.0320
V_{15}, p.u.	1.0034	V_{74}, p.u.	1.0232	T_{102}	1.0137
V_{18}, p.u.	0.9773	V_{76}, p.u.	1.0015	T_{107}	0.9795
V_{19}, p.u.	1.0324	V_{77}, p.u.	1.0124	T_{127}	0.9985
V_{24}, p.u.	1.0285	V_{80}, p.u.	1.0226	Capacitor banks	
V_{25}, p.u.	0.9705	V_{85}, p.u.	1.0117	$Q_{C\text{-}5}$, p.u.	−0.2403
V_{26}, p.u.	1.0175	V_{87}, p.u.	1.0058	$Q_{C\text{-}34}$, p.u.	0.0371
V_{27}, p.u.	1.0117	V_{89}, p.u.	1.0076	$Q_{C\text{-}37}$, p.u.	−0.0437
V_{31}, p.u.	1.0014	V_{90}, p.u.	0.9753	$Q_{C\text{-}44}$, p.u.	0.0375
V_{32}, p.u.	0.9988	V_{91}, p.u.	0.9836	$Q_{C\text{-}45}$, p.u.	0.0400
V_{34}, p.u.	1.0158	V_{92}, p.u.	1.0272	$Q_{C\text{-}46}$, p.u.	0.0749
V_{36}, p.u.	0.9916	V_{99}, p.u.	0.9612	$Q_{C\text{-}48}$, p.u.	0.0796
V_{40}, p.u.	1.0132	V_{100}, p.u.	1.0032	$Q_{C\text{-}74}$, p.u.	0.0883
V_{42}, p.u.	0.9892	V_{103}, p.u.	0.9843	$Q_{C\text{-}79}$, p.u.	0.1218
V_{46}, p.u.	1.0607	V_{104}, p.u.	0.9880	$Q_{C\text{-}82}$, p.u.	0.0380
V_{49}, p.u.	1.0031	V_{105}, p.u.	1.0003	$Q_{C\text{-}83}$, p.u.	0.0627
V_{54}, p.u.	1.0236	V_{107}, p.u.	1.0033	$Q_{C\text{-}105}$, p.u.	0.0830
V_{55}, p.u.	1.0176	V_{110}, p.u.	1.0040	$Q_{C\text{-}107}$, p.u.	0.0459
V_{56}, p.u.	1.0149	V_{111}, p.u.	1.0331	$Q_{C\text{-}110}$, p.u.	0.0221
V_{59}, p.u.	1.0584	V_{112}, p.u.	0.9877	P_{Loss}, MW	157.72
V_{61}, p.u.	0.9829	V_{113}, p.u.	0.9705	TVD, p.u.	**0.3666**
V_{62}, p.u.	1.0562	V_{116}, p.u.	1.0270	*L*-index, p.u.	0.1562
				CPU time, s	1121.17

tap-setting limits are taken from [20]. The system loads are given as follows: P_{Load} = 42.4200 p.u., Q_{Load} = 14.3800 p.u. The initial total generations and power losses are as follows: P_G = 43.7536 p.u., Q_G = 8.8192 p.u., P_{Loss} = 1.33357 p.u., Q_{Loss} = −7.8511 p.u.

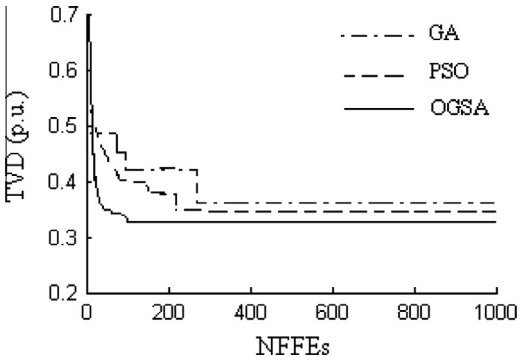

Fig. 8. Comparative convergence profiles of TVD for IEEE 118-bus test power system.

Table 12
Comparison of simulation results for IEEE 118-bus test power system with improvement of VSI.

Variable	OGSA	Variable	OGSA	Variable	OGSA
Generator voltage				Transformer tap ratio	
V_1, p.u.	0.9881	V_{65}, p.u.	1.0194	T_8	0.9621
V_4, p.u.	0.9924	V_{66}, p.u.	0.9525	T_{32}	1.0749
V_6, p.u.	0.9873	V_{69}, p.u.	0.9553	T_{36}	1.0149
V_8, p.u.	0.9984	V_{70}, p.u.	0.9818	T_{51}	0.9910
V_{10}, p.u.	1.0138	V_{72}, p.u.	1.0314	T_{93}	1.0871
V_{12}, p.u.	0.9855	V_{73}, p.u.	1.0161	T_{95}	0.9121
V_{15}, p.u.	1.0314	V_{74}, p.u.	1.0002	T_{102}	1.0637
V_{18}, p.u.	1.0373	V_{76}, p.u.	1.0100	T_{107}	0.9049
V_{19}, p.u.	1.0211	V_{77}, p.u.	1.0057	T_{127}	0.9848
V_{24}, p.u.	1.0294	V_{80}, p.u.	0.9844	Capacitor banks	
V_{25}, p.u.	1.0515	V_{85}, p.u.	1.0006	$Q_{C\text{-}5}$, p.u.	−0.3071
V_{26}, p.u.	1.0260	V_{87}, p.u.	0.9520	$Q_{C\text{-}34}$, p.u.	0.0165
V_{27}, p.u.	1.0306	V_{89}, p.u.	1.0661	$Q_{C\text{-}37}$, p.u.	−0.1891
V_{31}, p.u.	1.0307	V_{90}, p.u.	1.0152	$Q_{C\text{-}44}$, p.u.	0.0814
V_{32}, p.u.	1.0601	V_{91}, p.u.	0.9565	$Q_{C\text{-}45}$, p.u.	0.0777
V_{34}, p.u.	1.0587	V_{92}, p.u.	1.0172	$Q_{C\text{-}46}$, p.u.	0.0454
V_{36}, p.u.	1.0211	V_{99}, p.u.	0.9802	$Q_{C\text{-}48}$, p.u.	0.0042
V_{40}, p.u.	1.0356	V_{100}, p.u.	1.0461	$Q_{C\text{-}74}$, p.u.	0.1078
V_{42}, p.u.	1.0734	V_{103}, p.u.	1.0864	$Q_{C\text{-}79}$, p.u.	0.1361
V_{46}, p.u.	1.0989	V_{104}, p.u.	0.9825	$Q_{C\text{-}82}$, p.u.	0.1391
V_{49}, p.u.	1.0442	V_{105}, p.u.	1.0158	$Q_{C\text{-}83}$, p.u.	0.0434
V_{54}, p.u.	1.0827	V_{107}, p.u.	1.0087	$Q_{C\text{-}105}$, p.u.	0.0991
V_{55}, p.u.	1.0943	V_{110}, p.u.	1.0538	$Q_{C\text{-}107}$, p.u.	0.0520
V_{56}, p.u.	0.9575	V_{111}, p.u.	1.0403	$Q_{C\text{-}110}$, p.u.	0.0164
V_{59}, p.u.	0.9519	V_{112}, p.u.	0.9941	P_{Loss}, MW	295.1122
V_{61}, p.u.	0.9569	V_{113}, p.u.	1.0455	TVD, p.u.	1.4804
V_{62}, p.u.	1.0869	V_{116}, p.u.	1.0751	*L*-index, p.u.	0.0600
				CPU time, s	1112.19

5.3.1. Minimization of system P_{Loss} for IEEE 118-bus power system

OGSA-based reactive power dispatch schedule for the test system of P_{Loss} minimization objective is presented in Table 9 and the results obtained are compared to GSA [20], CLPSO [41] and PSO [41]. This table demonstrates that the OGSA yields optimal P_{Loss} as compared to other algorithms.

Table 10 shows the statistical comparison of results obtained by OGSA, GSA [20], CLPSO [41] and PSO [41] methods as regards to the objective function of minimizing P_{Loss} only. From this table it is observed that execution time of OGSA is the least one among the reported algorithms. From this table it may also be noted that the standard deviation and median values are quite satisfactory for OGSA. Success rate of OGSA may also be found to be promising one. The results in this table clearly indicate the superiority of OGSA over either GSA or PSO or CLPSO.

Fig. 7 shows the variation of the P_{Loss} (MW) against NFFEs for this test case for GA-, PSO- and OGSA-based approaches. Good

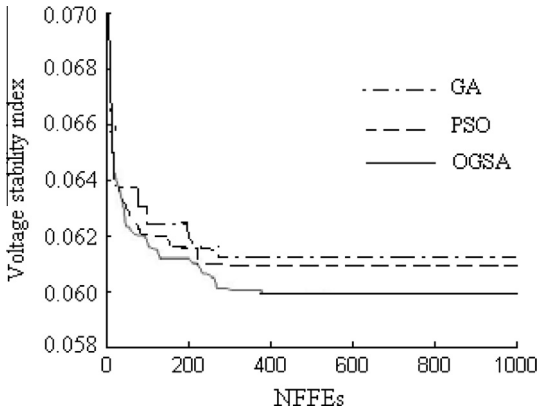

Fig. 9. Comparative convergence profiles of voltage stability index for IEEE 118-bus test power system.

convergence profile of OGSA may be noted from this figure by means of its ability to reach the near optimal solution.

5.3.2. Minimization of system TVD for IEEE 118-bus power system

The best reactive power dispatch solutions as yielded by the proposed OGSA from 30 runs for TVD objective function minimization objective are tabulated in Table 11. Comparative GA-, PSO- and OGSA-based convergence profiles of TVD (p.u.) for this test power system is presented in Fig. 8. From this figure it may be observed that the convergence profile of TVD (p.u.) for the proposed OGSA-based approach for this test system is promising one.

5.3.3. Improvement of VSI for IEEE 118-bus power system

The best reactive power dispatch solutions as yielded by the proposed OGSA from 30 runs for VSI objective function minimization objective are tabulated in Table 12. Comparative GA-, PSO- and OGSA-based convergence profiles of VSI for this test power system is presented in Fig. 9. From this figure it may be observed that the convergence profile of voltage stability index for the proposed OGSA-based approach for this test system is promising one.

5.4. Robustness study against control parameters

The performance of any evolutionary algorithm largely depends on the right selection of its control parameters. The performance of the OGSA also depends on the selection of values of G_0, τ and J_r. In the present work, a robustness study is carried out on IEEE 30-bus power system with transmission loss minimization objective. The known minimum solution for this problem from the literature is 4.514310 MW [20]. Different sets of parameters are tried to find a result better than this one. The effects of parameters in OGSA are illustrated in Tables 13 and 14, where 100 random trial runs

Table 13
Effect of G_0 and τ on the performance of OGSA for IEEE 30-bus test power system with P_{Loss} minimization objective.

Case	G_0	Minimal P_{Loss} (MW)	Success rate if τ is				
			1	5	**10**	15	20
1	25	4.4984	9	17	17	11	10
2	50	4.4984	19	18	21	10	9
3	75	4.4984	12	10	10	15	8
4	**100**	4.4984	14	25	**66**	19	7
5	125	4.4984	13	16	11	10	16
6	150	4.4984	14	15	18	19	14
7	175	4.4984	15	10	17	18	17
8	200	4.4984	12	13	16	21	19

Table 14
Effect of J_r on the performance of OGSA for IEEE 30-bus test power system with P_{Loss} minimization objective.

Case	Minimal P_{Loss} (MW)	Success rate if J_r is								
		0.1	0.2	0.3	0.4	0.5	0.6	0.7	0.8	0.9
1	4.4984	15	19	**58**	18	17	13	12	11	7

are performed for each parameter set. The value of NFFEs is set as 1000. Among the different set of parameters (like G_0 and τ) for OGSA algorithm, Case 4 in Table 13 shows the best performance in terms of the highest number of hits to minimum solution. Thus, the values of G_0 and τ are selected as 100 and 10, respectively. Similarly, Table 14 shows the best performance of the algorithm when the value of J_r is selected as 0.3. Thus, these values of the parameters are subsequently selected for all the test cases of the current paper.

6. Conclusion

In this paper, one recently developed meta-heuristic like OGSA has been, successfully, implemented to solve the ORPD problem of power systems and the economical (in the form of minimization of active power loss) as well as technical (in the form of minimization of TVD or improvement of VSI) benefits arisen are presented. The ORPD problem is formulated as a nonlinear optimization problem with equality and inequality constraints of the power network. In this study, minimization of active power loss, or that of TVD, or improvement of VSI are, individually, considered. The proposed OGSA is tested on IEEE 30-, 57-, and 118-bus test power systems to demonstrate its effectiveness. From the simulation work, it is observed that the proposed OGSA yields optimal settings of the control variables of the test power system. The simulation results also indicate the robustness and superiority of the proposed approach to solve the ORPD problem of power systems. It is noticed that the concept of opposition-based learning in GSA for population initialization and also for generation jumping enhances its optimization capability in terms of its searching capability and robustness as compared to the basic GSA counterpart. The results obtained from the simulation of the present paper obviously demonstrate that the proposed OGSA yields better-quality solution in comparison to the GSA-based results previously reported in the recent state-of-the-art literature. Thus, the proposed OGSA may be recommended as a very promising algorithm for solving some more other complex engineering optimization problems for the future researchers.

References

[1] Durairaj S, Kannan PS, Devaraj D. Multi-objective VAR dispatch using particle swarm optimization. Emerg Electr Power Syst 2005;4(1). ISSN(online):1553-779X.
[2] Happ HH. Optimal power dispatch – a comprehensive survey. IEEE Trans Power Apparat Syst 1977;PAS-96:841–51.
[3] Momoh JA, El-Hawary ME, Adapa R. A review of selected optimal power flow literature to 1993 part I & II. IEEE Trans Power Syst 1999;14(1):96–111.
[4] Granville S. Optimal reactive dispatch through interior point methods. IEEE IEEE Trans Power Syst 1994;9(1):136–46.
[5] Quintana VH, Santos-Nieto M. Reactive power-dispatch by successive quadratic programming. IEEE Trans Energy Convers 1989;4(3):425–35.
[6] Ramos JLM, Exposito AG, Quintana VH. Transmission power loss reduction by interior-point methods: implementation issues and practical experience. IEE Proc Gen Trans Distrib 2005;152(1):90–8.
[7] Bakare GA, Venayagamoorthy GK, Aliyu UO. Reactive power and voltage control of the Nigerian grid system using microgenetic algorithm. In: Proc IEEE power eng soc general meeting; 2005. p. 1916–22.
[8] Durairaj S, Devaraj D, Kannan PS. Genetic algorithm applications to optimal reactive power dispatch with voltage stability enhancement. IE (I) J-EL 2006;87:42–7.

[9] Devaraj D. Improved genetic algorithm for multi-objective reactive power dispatch problem. Eur Trans Electr Power 2007;17:569–81.
[10] Devaraj D, Durairaj S, Kannan PS. Real parameter genetic algorithm to multi-objective reactive power dispatch. Int J Power Energy Syst 2008;28(1):1710–2243.
[11] Wu QH, Cao YJ, Wen JY. Optimal reactive power dispatch using an adaptive genetic algorithm. Int J Electr Power Energy Syst 1998;20(8):563–9.
[12] Wu QH, Ma JT. Power system optimal reactive power dispatch using evolutionary programming. IEEE Trans Power Syst 1995;10(3):1243–9.
[13] Yoshida H, Kawata K, Fukuyama Y, Takamura S, Nakanishi Y. A particle swarm optimization for reactive power and voltage control considering voltage security assessment. IEEE Trans Power Syst 2000;15(4):1232–9.
[14] Esmin AAA, Lambert-Torres G, De-Souza ACZ. A hybrid particle swarm optimization applied to loss power minimization. IEEE Trans Power Syst 2005;20(2):859–66.
[15] Tripathy M, Mishra S. Bacteria foraging-based solution to optimize both real power loss and voltage stability limit. IEEE Trans Power Syst 2007;22(1):240–8.
[16] Ela AAAE, Abido MA, Spea SR. Differential evolution algorithm for optimal reactive power dispatch. Electr Power Syst Res 2011;81:458–64.
[17] Liang CH, Chung CY, Wong KP, Duan XZ, Tse CT. Study of differential evolution for optimal reactive power flow. IEE Proc Gen Trans Distrib 2007;1(2):253–60.
[18] Varadarajan M, Swarup KS. Network loss minimization with voltage security using differential evolution. Electr Power Syst Res 2008;78:815–23.
[19] Dai C, Chen W, Zhu Y, Zhang X. Seeker optimization algorithm for optimal reactive power dispatch. IEEE Trans Power Syst 2009;24(3):1218–31.
[20] Duman S, So¨nmez Y, Gu¨venc U, Yo¨ru¨keren N. Optimal reactive power dispatch using a gravitational search algorithm. IET Gener Transm Distrib 2012;6(6):563–76.
[21] Zhang J, Sanderson AC. JADE: adaptive differential evolution with optional external archive. IEEE Trans Evol Compt 2009;13(5):945–58.
[22] Lampinen J, Zelinka I. On stagnation of the differential evolution algorithms. In: Proc 6th int conf, soft computing; 2000. p. 76–83.
[23] Rashedi E, Nezamabadi-pour H, Saryazdi S. GSA: a gravitational search algorithm. Inf Sci 2009;179(13):2232–48.
[24] Tizhoosh HR. Opposition-based learning: a new scheme for machine intelligence. In: Proc int conf computational intel, modeling, control and automation; 2005. p. 695–701.
[25] Rahnamayan S, Tizhoosh HR, Salama MMA. Opposition-based differential evolution. IEEE Trans Evol Comput 2008;12(1):64–79.
[26] Shaw B, Mukherjee V, Ghoshal SP. A novel opposition-based gravitational search algorithm for combined economic and emission dispatch problems of power systems. Int J Electr Power Energy Syst 2012;35(1):21–33.
[27] Chatterjee A, Ghoshal SP, Mukherjee V. Solution of combined economic and emission dispatch problems of power systems by an opposition-based harmony search algorithm. Int J Electr Power Energy Syst 2012;39(1):9–20.
[28] Halliday D, Resnick R, Walker J. Fundamentals of physics. New York: John Wiley and Sons; 1993.
[29] Yin M, Hu Y, Yang F, Li X, Gu W. A novel hybrid K-harmonic means and gravitational search algorithm approach for clustering. Expert Syst Appl 2011;38(8):9319–24.
[30] Sarafrazi S, Nezamabadi-pour H, Saryazdi S. Disruption: a new operator in gravitational search algorithm. Scientia Iranica 2011;18(3):539–48.
[31] Sarafrazi S, Nezamabadi-pour H. Facing the classification of binary problems with a GSA-SVM hybrid system. Math Comp Model 2013;57(1–2):270–8.
[32] Sun G, Liu Q, Ji C, Li X. A novel approach for edge detection based on the theory of universal gravity. Pattern Recogn 2007;40(10):2766–75.
[33] Lopez-Molina C, Bustince H, Fernandez J, Couto P, Baets B. A gravitational approach to edge detection based on triangular norms. Pattern Recogn 2010;43(11):3730–41.
[34] Rashedi E, Nezamabadi-pour H, Saryazdi S. Filter modeling using gravitational search algorithm. Eng Appl Artif Intel 2011;24(1):117–22.
[35] Li C, Zhou J. Parameters identification of hydraulic turbine governing system using improved gravitational search algorithm. Energy Convers Manage 2001;52(4):374–81.
[36] Precup RE, David RC, Petriu EM, Radac MB, Preitl S, Fodor J. Evolutionary optimization-based tuning of low-cost fuzzy controllers for servo systems. Knowledge-Based Syst 2011;38:74–84.
[37] Behrang MA, Assareh E, Ghalambaz M, Assari MR, Noghrehabadi AR. Forecasting future oil demand in Iran using GSA (Gravitational Search Algorithm). Energy 2011;36(9):5649–54.
[38] Ali Ghasemi, Hossein Shayeghi, Hasan Alkhatib. Robust design of multimachine power system stabilizers using fuzzy gravitational search algorithm. Int J Electr Power Energy Syst 2013;51:190–200.
[39] Wang XF, Song Y, Irving M. Modern power systems analysis. New York: Springer; 2008.
[40] Bhattacharya A, Chattopadhyay PK. Solution of optimal reactive power flow using biogeography-based optimization. Int J Electr Electron Eng 2010;4(8):568–76.
[41] Mahadevan K, Kannan PS. Comprehensive learning particle swarm optimization for reactive power dispatch. Appl Soft Comput 2010;10:641–52.
[42] Subbaraj P, Rajnarayanan PN. Optimal reactive power dispatch using self-adaptive real coded genetic algorithm. Electr Power Syst Res 2009;79:374–81.
[43] Zimmerman RD, Murillo-Sanchez CE, Gan D. Matlab power system simulation package (Version 3.1b2); 2006. <http://www.pserc.cornell.edu/matpower/>.
[44] The IEEE 57-bus test system. <http://www.ee.washington.edu/research/pstca/pf57/pg_tca57bus.htm>.
[45] The IEEE 118-bus test system. <http://www.ee.washington.edu/research/pstca/pf118/pg_tca118bus.htm>.
[46] Jeyadevi S, Baskar S, Babulal CK, Iruthayarajan MW. Solving multiobjective optimal reactive power dispatch using modified NSGA-II. Int J Electr Power Energy Syst 2011;33(2):219–28.